

Pneumococcal meningitis is promoted by single cocci expressing pilus-adhesin RrgA

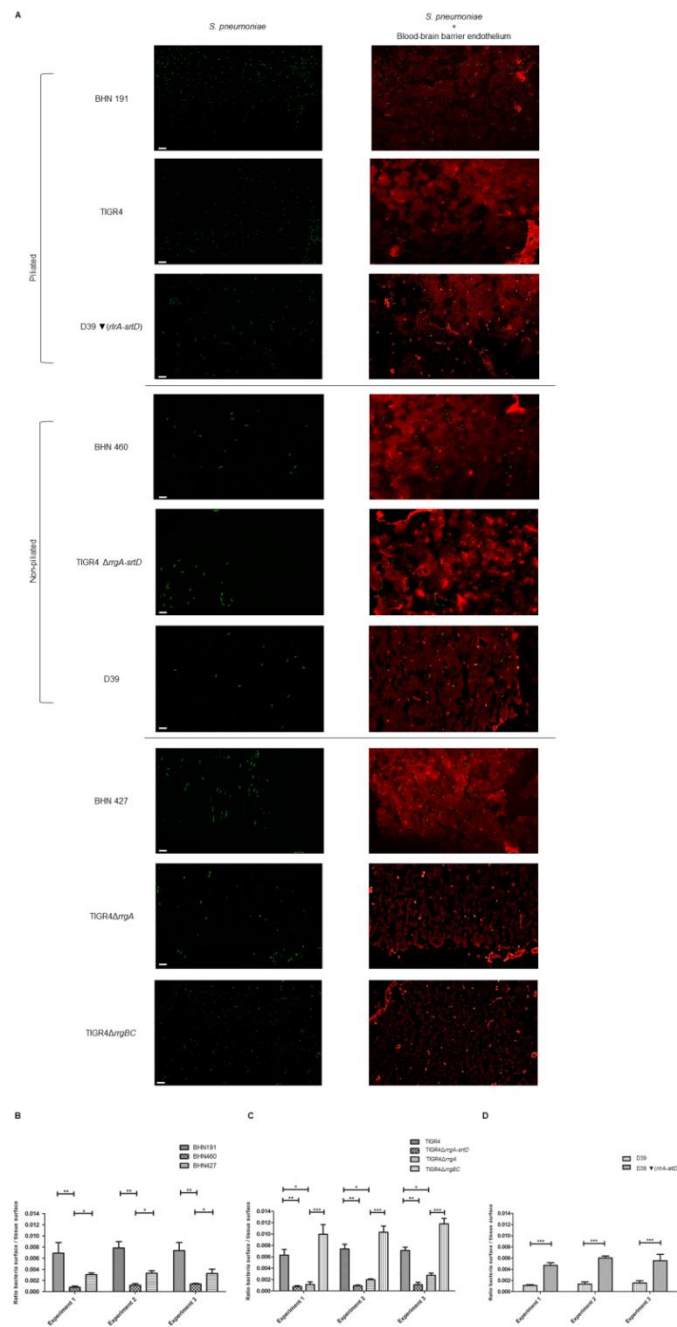
Federico Iovino ¹, Disa L. Hammarlöf ^{1,2}, Genevieve Garriss ¹, Sarah Browall ¹, Priyanka Nannapaneni ¹, Birgitta Henriques-Normark ¹

1. Department of Microbiology, Tumor and Cell Biology, Karolinska Institutet, SE-171 77 Stockholm Sweden, and Department of Clinical Microbiology, Karolinska University Hospital, SE-171 76 Stockholm, Sweden
2. Current address: Department of Cell and Molecular Biology, Uppsala Universitet, SE- 751 24, Uppsala, Sweden

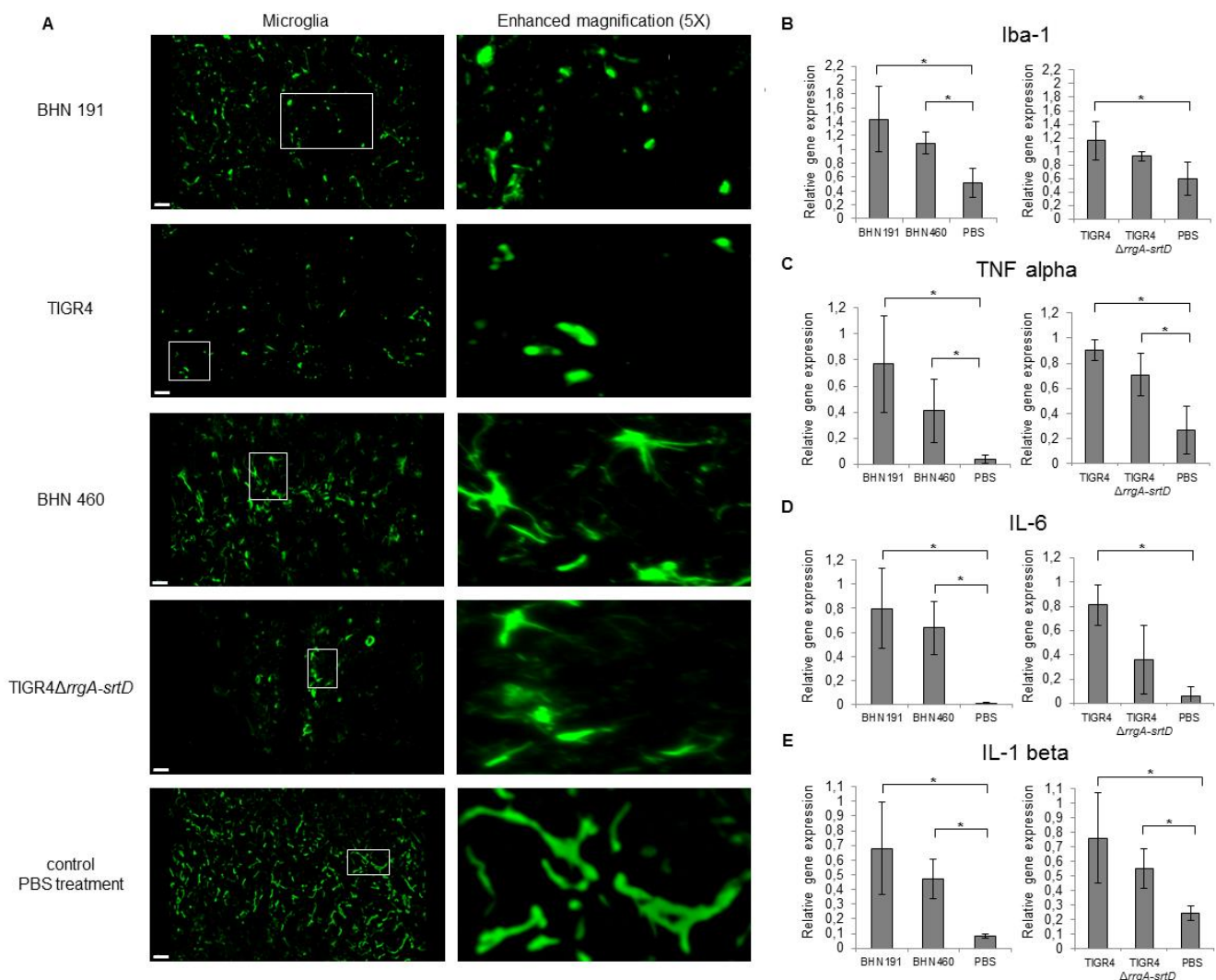
Supplemental Data

Supplemental Figure 1. Bioinformatic alignment of genomic sequences from the serotype 6B clinical isolates. (A) The alignment of the genomic sequences shows that the *rlrA* operon is expressed in the clinical isolates BHN191 and BHN427, while it is absent in BHN460. (B) Sequence analysis of the pilus region shows that BHN191 and BHN427 are identical except for the deletion of 10bp (ATACTATACT) in BHN427 upstream of the translational start site for the *rrgA* gene.

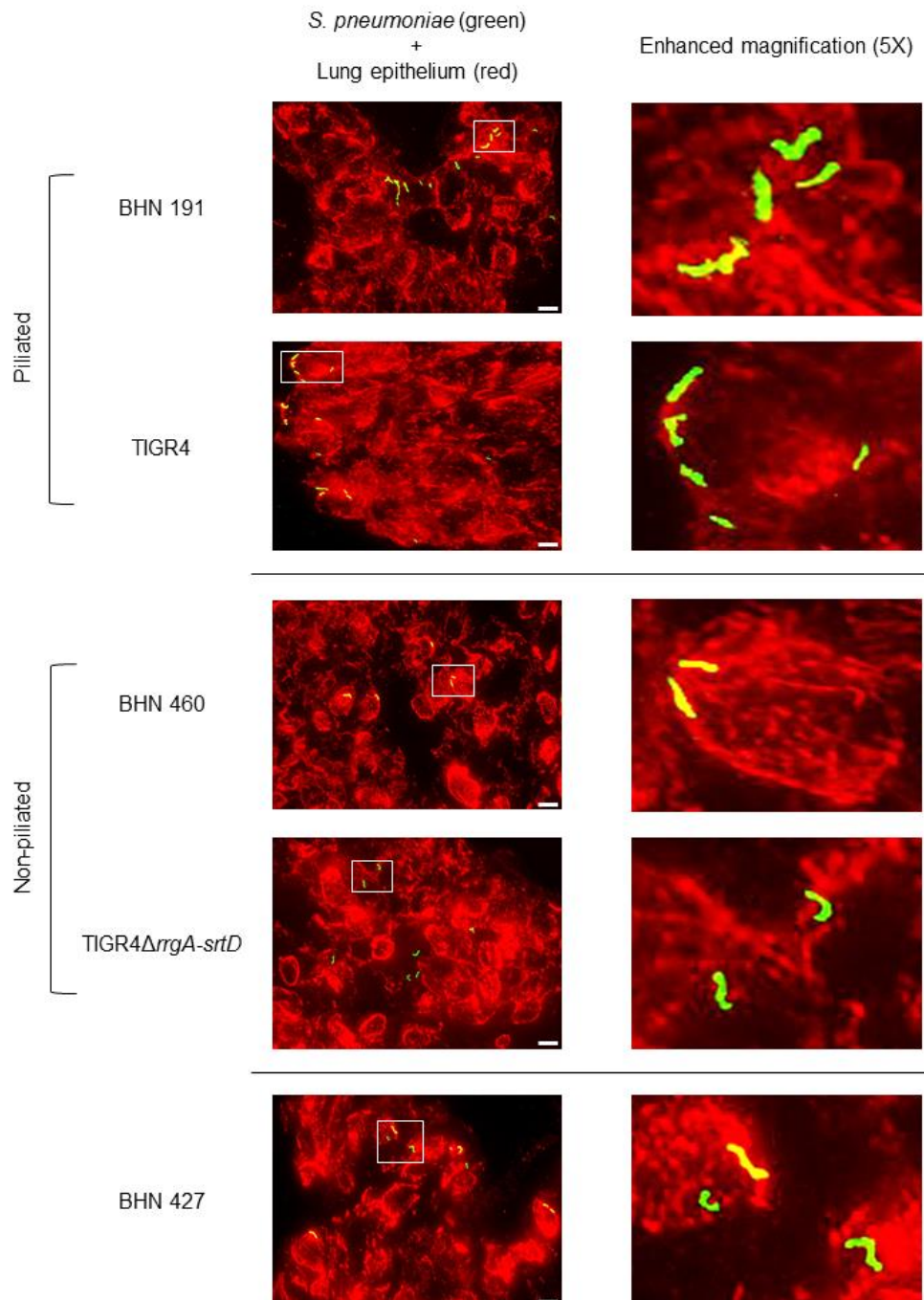
Supplemental Figure 2. Quantification of pneumococci in the brain. (A) Visualization of *S. pneumoniae* in brain tissue sections with low magnification (10X objective); each image represents ¼ of an entire brain section. The scale bar represents 20 µm. (B-D) Quantification of the total amount of bacteria in the brain of mice infected with the three serotype 6B clinical isolates BHN191, BHN460, BHN427 (B), with TIGR4, TIGR4Δ*rrgA-srtD*, TIGR4Δ*rrgBC* and TIGR4Δ*rrgA* (C), and with D39 and D39▼(*rlrA-srtD*). Tissue sections from 3 mice were imaged for each group using 6 brain sections per mouse (in A one representative image per each strain is shown); the averages of each group (calculated with the average values of each mouse in each group) ± SD were calculated for the final quantification. In B-D the nonparametric ANOVA test combined with the Dunn's test were used, * indicates p<0.05, ** indicates p<0.01, *** indicates p<0.001.



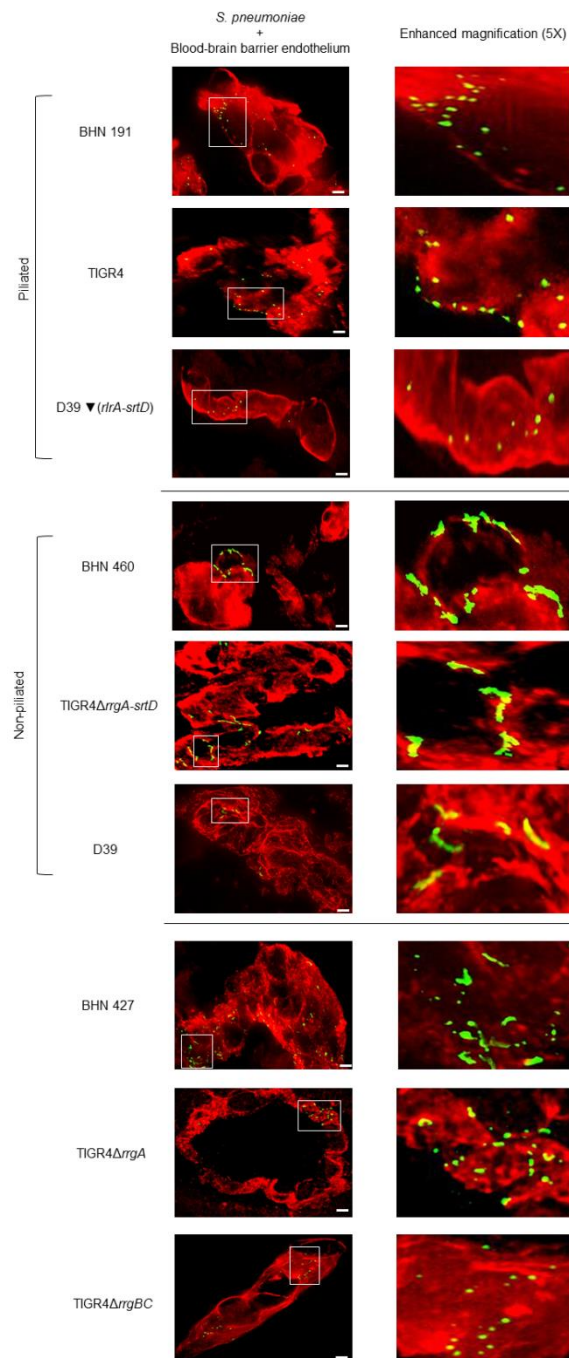
Supplemental Figure 3. Pneumococcal pilus-1 enhances neuroinflammation. (A) Neuroinflammation was assessed by studying morphology of microglia. The scale bar represents 20 μm ; the panel "Enhanced magnification" shows microglia within white rectangles with higher magnification. One representative image per each strain is shown, in total tissue sections from 3 mice were analyzed for each strain using 6 tissue sections per mouse. (B-E) Relative gene expression of Iba-1, TNF alpha, IL-6 and IL-1beta in the brain normalized to expression of the house-keeping gene *GAPDH*. In B-E the nonparametric ANOVA test combined with the Dunn's test were used, * $p < 0.05$; in each biological replicate the average value out of three mice was calculated per strain, in the graph each column represents the final average that was calculated using the average values of each biological replicate (= three average values), SD is the deviation of the three average values.



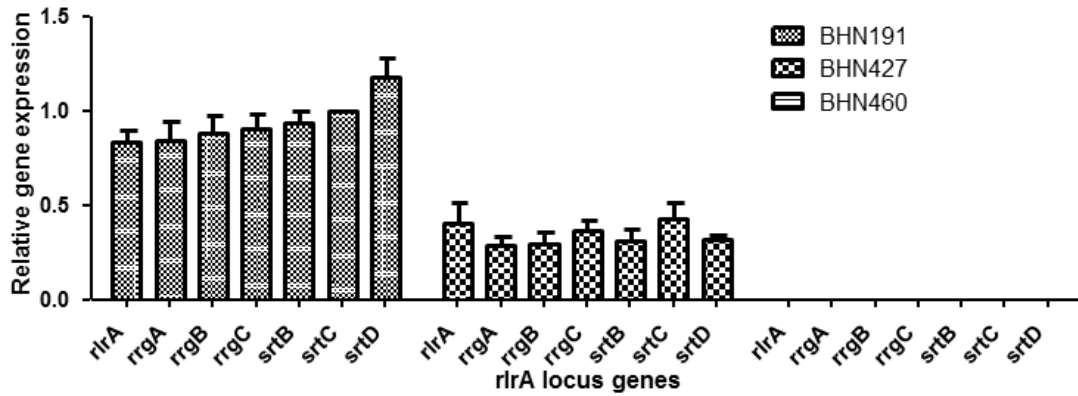
Supplemental Figure 4. Piliated and non-piliated pneumococci form chains in the lung tissue. Immunofluorescent staining of lung tissue sections showed that all five strains invade the lung epithelium in the form of chains. The white scale bar represents 10 μ m. In the panel “Enhanced magnification” the parts of image within the white rectangles are shown with higher magnification. One representative image for each strain is shown, in total tissue sections from 3 mice were analyzed for each strain using 6 tissue sections per mouse.



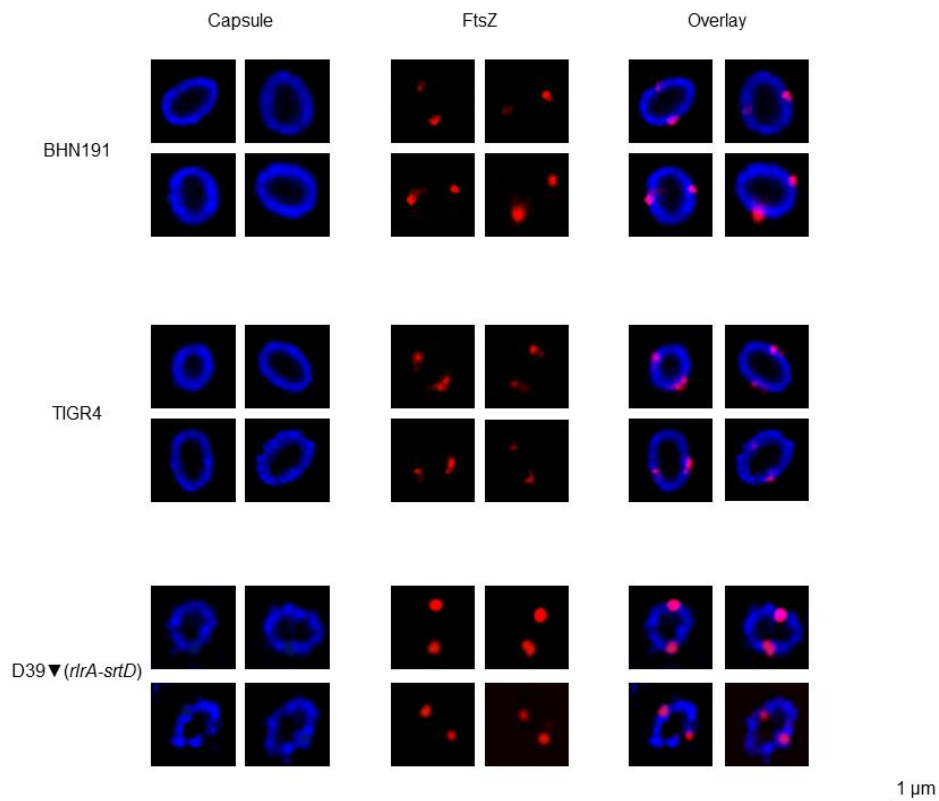
Supplemental Figure 5. Pneumococci carrying pilus 1 invade the brain as single cocci. Immunofluorescent staining of brain tissues showing pneumococci (green) crossing the BBB (red). The piliated strains BHN191, TIGR4, and D39 ∇ (*rtrA-srtD*) as well as the non-piliated but RrgA containing TIGR4 Δ *rrgBC* crossed the BBB as single cocci, while non-piliated BHN460, TIGR4 Δ *rrgA-srtD* and D39 formed chains. Piliated BHN427 and TIGR4 Δ *rrgA* formed a mixed population composed of chains of various length and single cocci. The white scale bar represents 10 μ m. The panel "Enhanced magnification" shows the parts within white rectangles with higher magnification. One representative image for each strain is shown, in total tissue sections from 3 mice were analyzed for each strain using 6 tissue sections per mouse.



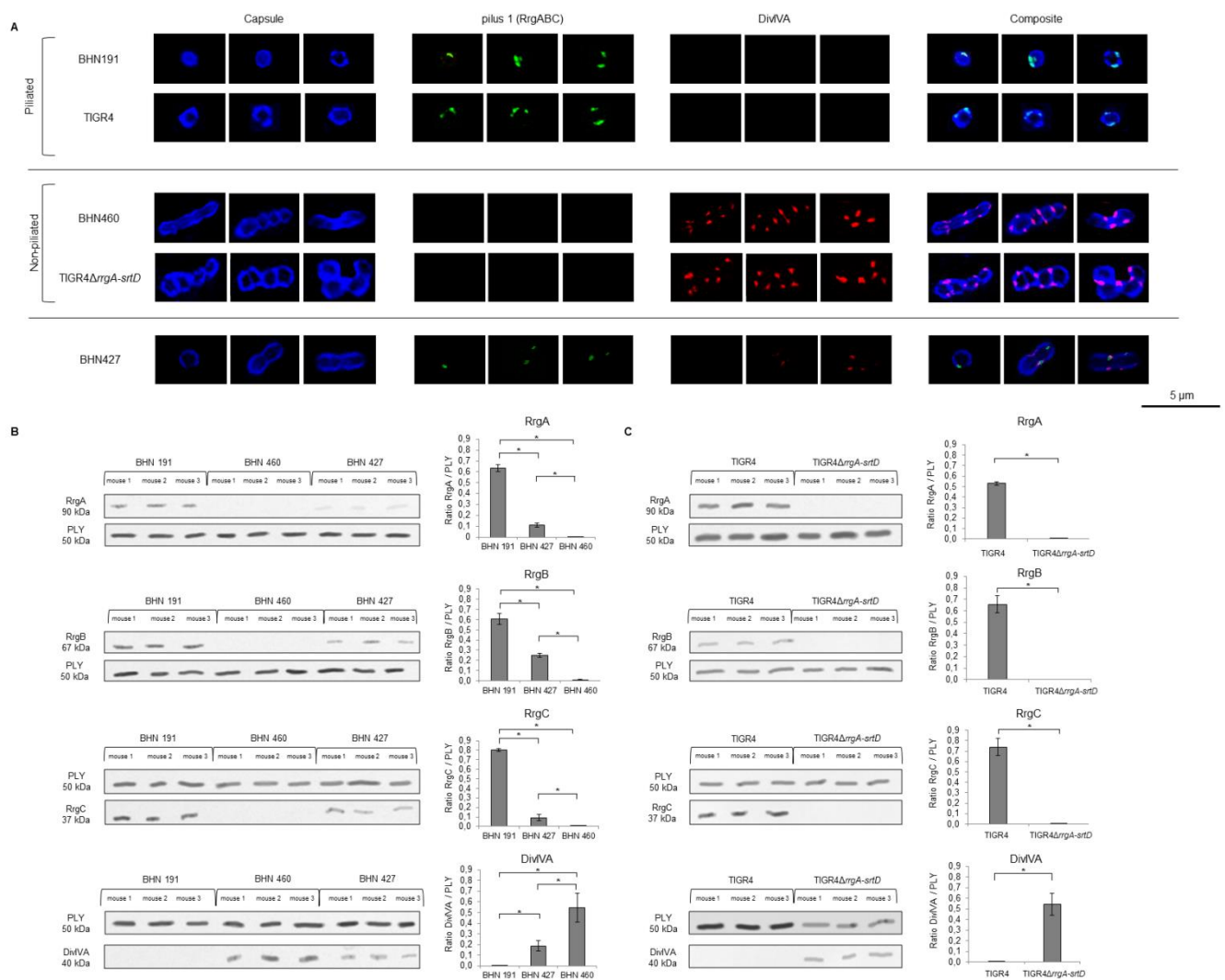
Supplemental Figure 6. Expression analyses of the structural pilus protein genes in pneumococci grown in vitro (THY medium). Expression analyses of the pilus protein genes in the serotype 6B isolates BHN191, BHN427 and BHN460. Relative expression of the regulator *rlrA* and the pilus protein genes was analyzed by qPCR, normalizing gene expression signals to expression of house-keeping gene *GAPDH*. The average values \pm SD were calculated using the average values of three biological replicates.



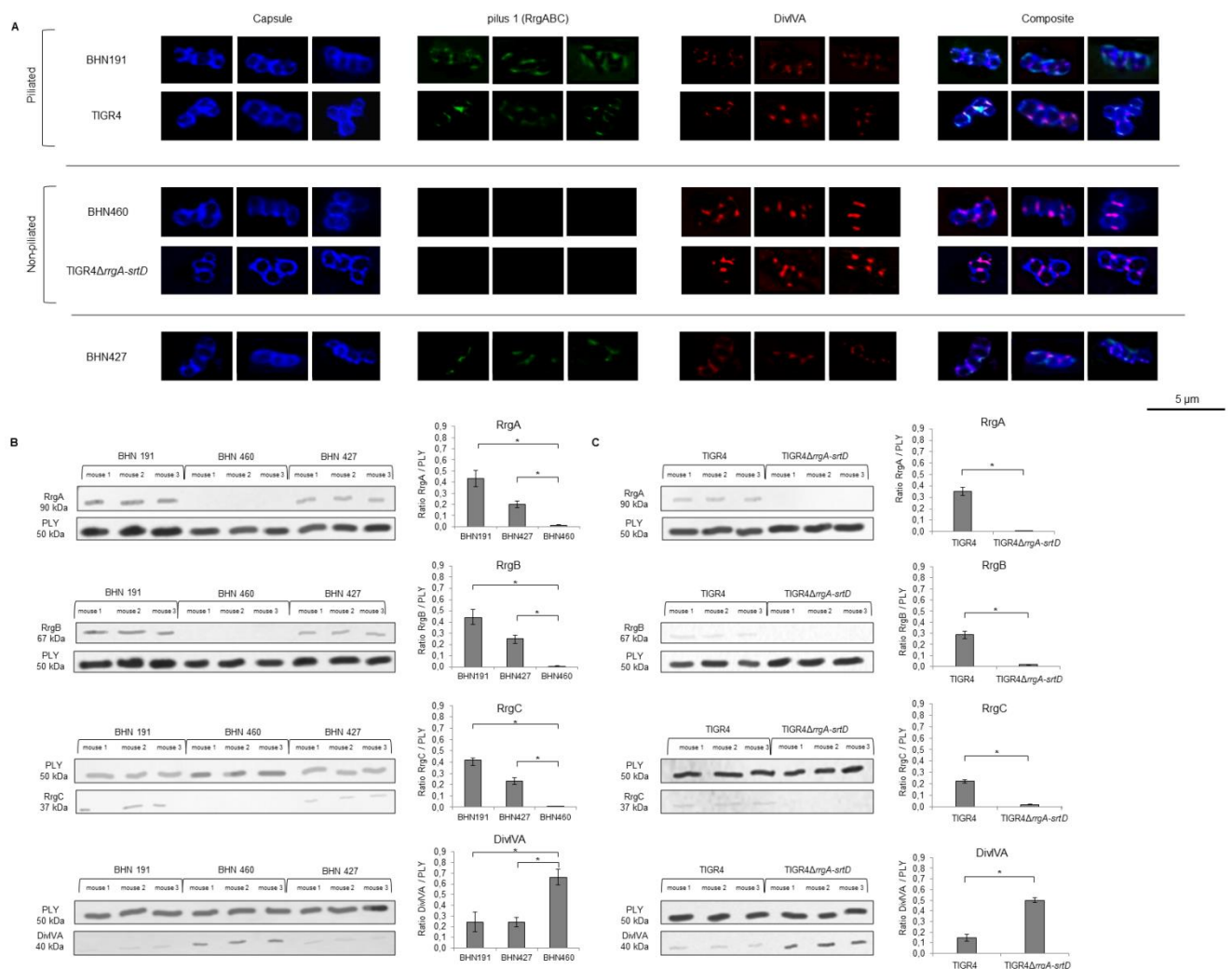
Supplemental Figure 7. Piliated single pneumococci are able to divide in the brain tissue. Immunofluorescence staining showing capsule (blue) and FtsZ (red) of piliated BHN191, TIGR4 and D39 ∇ (*rlrA-srtD*) in brain homogenates. 4 representative cocci/strain are shown, in total 900 single cocci/strain were imaged.



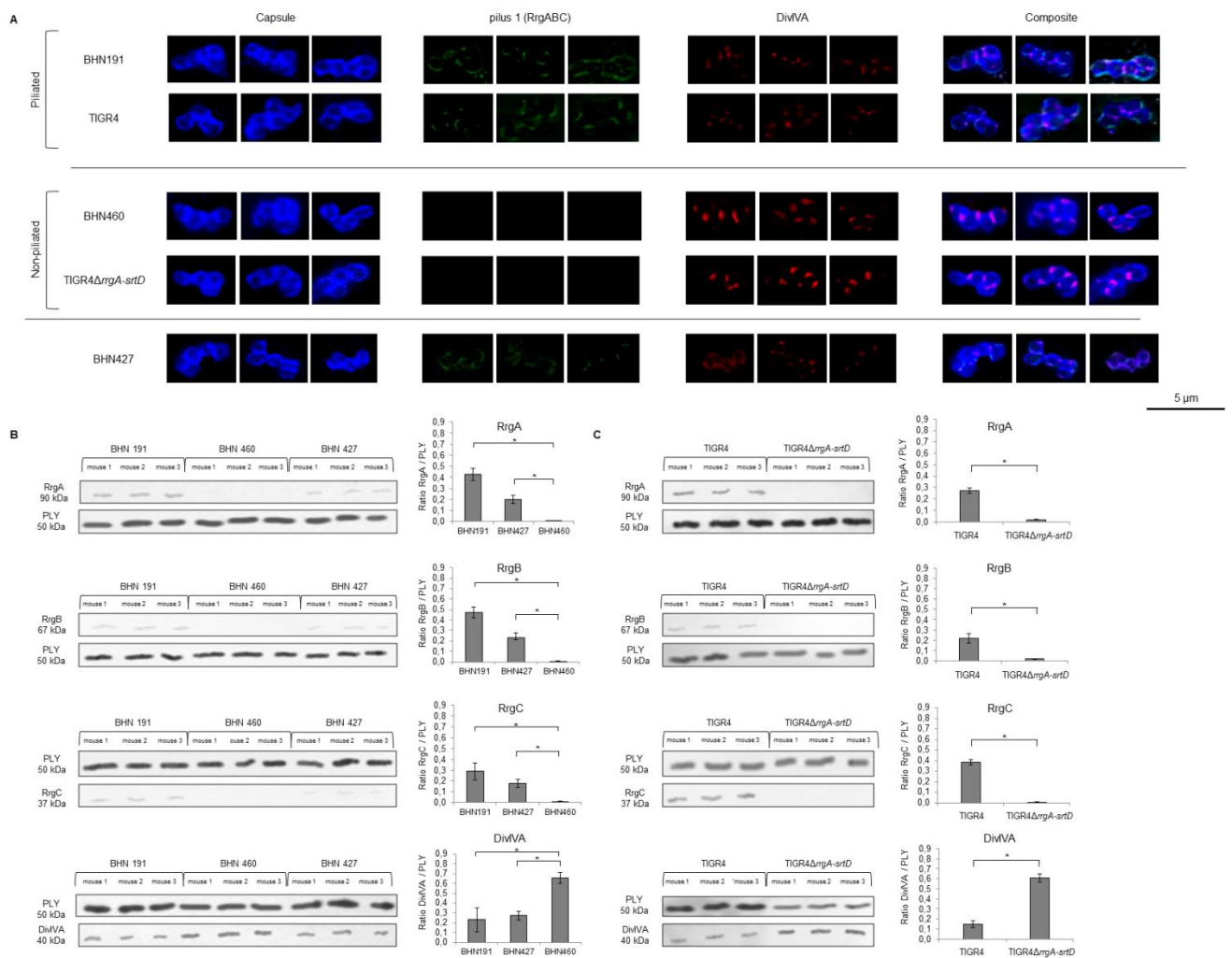
Supplementary Figure 8. Expression of pilus-1 and DivIVA in pneumococci recovered from brain tissue. (A) Immunofluorescent staining of the pneumococci from blood samples showing capsule (blue), pilus-1 (RrgA, RrgB and RrgC) (green) and DivIVA (red). For each strain, three representative bacteria are shown, in total approximately 900 bacteria/chains were imaged for each strain, 300 images/mouse and the three Div images that are shown are representative of the three mice that have been analyzed per group. (B, C) Western blot detection and protein quantification of RrgA, RrgB, RrgC and DivIVA expressed in (B) the three 6B clinical isolates, (C) TIGR4 and TIGR4 Δ *rrgA-srtD* in brain homogenates. In each biological replicate the average value out of three mice was calculated per strain; each column represents the final average that was calculated using the average values of each biological replicate (= three average values), SD is the deviation of the three average values; each biological replicate was performed using brain homogenates from 3 mice/strain, the results in the figures show one biological replicate as representative of the three replicates performed. In B the nonparametric ANOVA test combined with the Dunn's test were used, in C the non-parametric 2-tailed Wilcoxon's rank sum test was used, * $p < 0.05$.



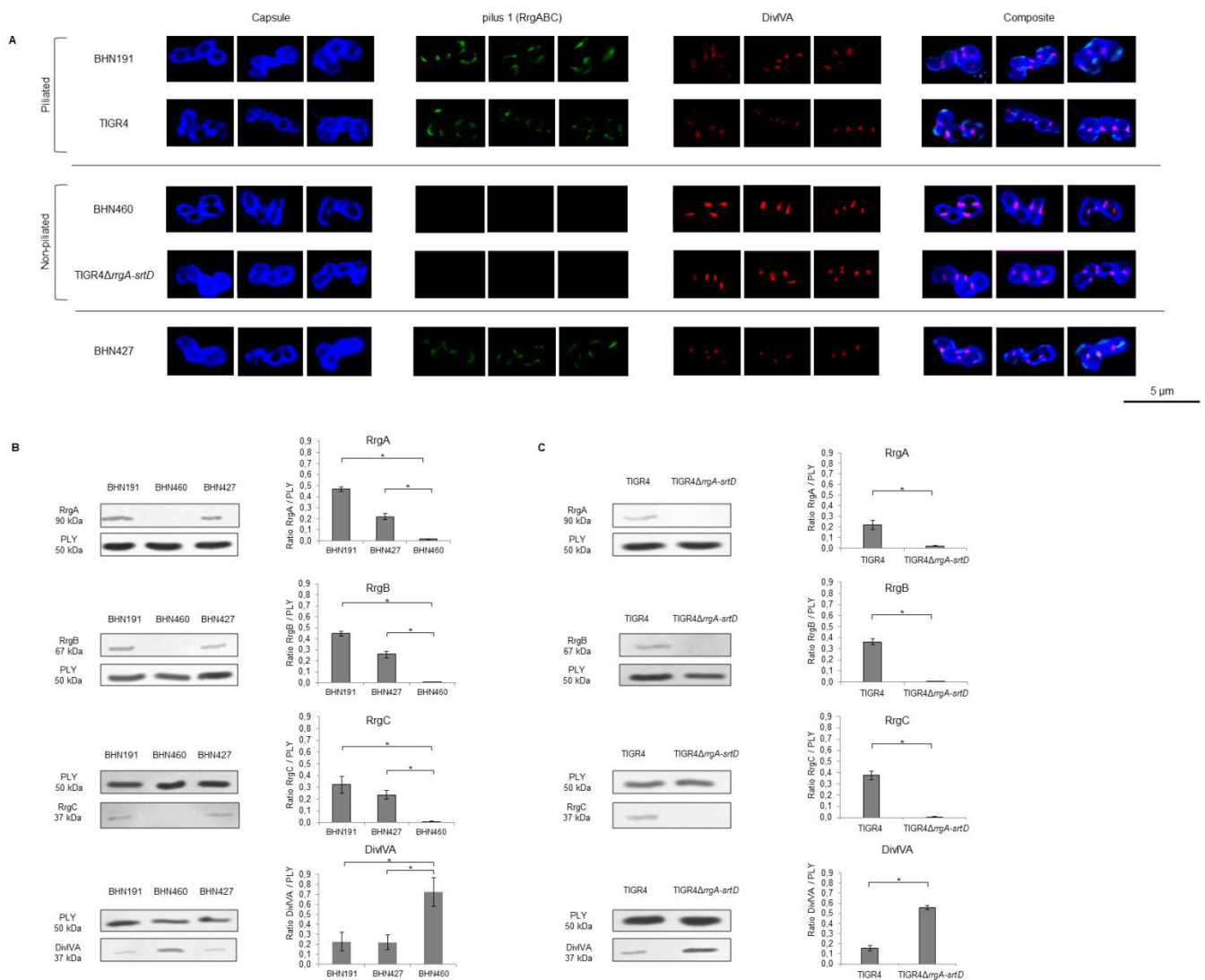
Supplemental Figure 9. Expression of pilus-1 and DivIVA in pneumococci isolated from the blood. (A) Immunofluorescent staining of the pneumococci from blood samples showing capsule (blue), pilus-1 (RrgA, RrgB and RrgC) (green) and DivIVA (red). For each strain, three representative bacteria are shown, in total approximately 900 bacteria/chains have been imaged for each strain, 300 images/mouse and the three images that are shown are representative of the three mice that have been analyzed per group. (B, C) Western blot detection and protein quantification of RrgA, RrgB, RrgC and DivIVA expressed in (B) the three 6B clinical isolates, (C) TIGR4 and TIGR4 Δ *rrgA-srtD* in blood samples. In each biological replicate the average value out of three mice was calculated per strain; each column represents the final average that was calculated using the average values of each biological replicate (= three average values), SD is the deviation of the three average values; each biological replicate was performed using brain homogenates from 3 mice/strain, the results in the figures show one biological replicate as representative of the three replicates performed. In B the nonparametric ANOVA test combined with the Dunn's test were used, in C the non-parametric 2-tailed Wilcoxon's rank sum test was used, * $p < 0.05$.



Supplemental Figure 10. Expression of pilus-1 and DivIVA in pneumococci recovered from lung tissue. (A) Immunofluorescent staining of the pneumococci in lung homogenates showing capsule (blue), pilus-1 (RrgA, RrgB and RrgC) (green) and DivIVA (red). For each strain, three representative bacteria are shown, in total approximately 900 bacteria/chains have been imaged for each strain, 300 images/mouse and the three images that are shown are representative of the three mice that have been analyzed per group. (B, C) Western blot detection and protein quantification of RrgA, RrgB, RrgC and DivIVA expressed in (B) the three 6B clinical isolates, (C) TIGR4 and TIGR4 Δ *rrgA-srtD* in lung homogenates. In each biological replicate the average value out of three mice was calculated per strain; each column represents the final average that was calculated using the average values of each biological replicate (= three average values), SD is the deviation of the three average values; each biological replicate was performed using brain homogenates from 3 mice/strain, the results in the figures show one biological replicate as representative of the three replicates performed. In B the nonparametric ANOVA test combined with the Dunn's test were used, in C the non-parametric 2-tailed Wilcoxon's rank sum test was used, * $p < 0.05$.

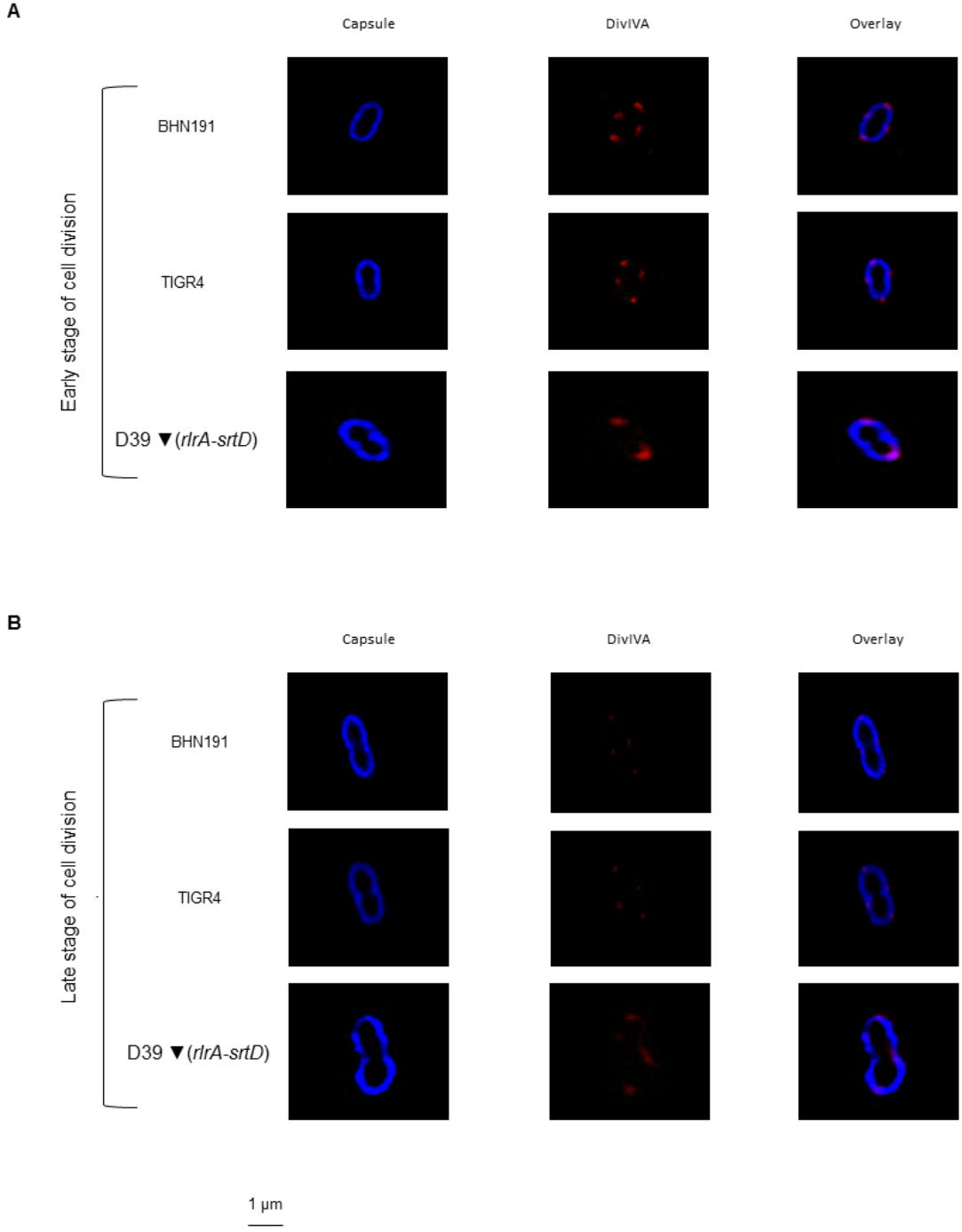


Supplemental Figure 11. Expression of pilus-1 and DivIVA in pneumococci grown in THY medium. (A) Immunofluorescent staining of the pneumococci in THY cultures showing capsule (blue), pilus-1 (RrgA, RrgB and RrgC) (green) and DivIVA (red). For each strain, three representative bacteria are shown, in total approximately 900 bacteria/chains have been imaged for each strain, 300 images/mouse and the three images that are shown are representative of the three mice that have been analyzed per group. (B, C) Western blot detection and protein quantification of RrgA, RrgB, RrgC and DivIVA expressed by (B) the 6B clinical isolates, (C) TIGR4 and TIGR4 Δ *rrgA-srtD* in THY cultures. In each biological replicate the average value out of three mice was calculated per strain; each column represents the final average that was calculated using the average values of each biological replicate (= three average values), SD is the deviation of the three average values; each biological replicate was performed using brain homogenates from 3 mice/strain, the results in the figures show one biological replicate as representative of the three replicates performed. In B the nonparametric ANOVA test combined with the Dunn's test were used, in C the non-parametric 2-tailed Wilcoxon's rank sum test was used, * $p < 0.05$.

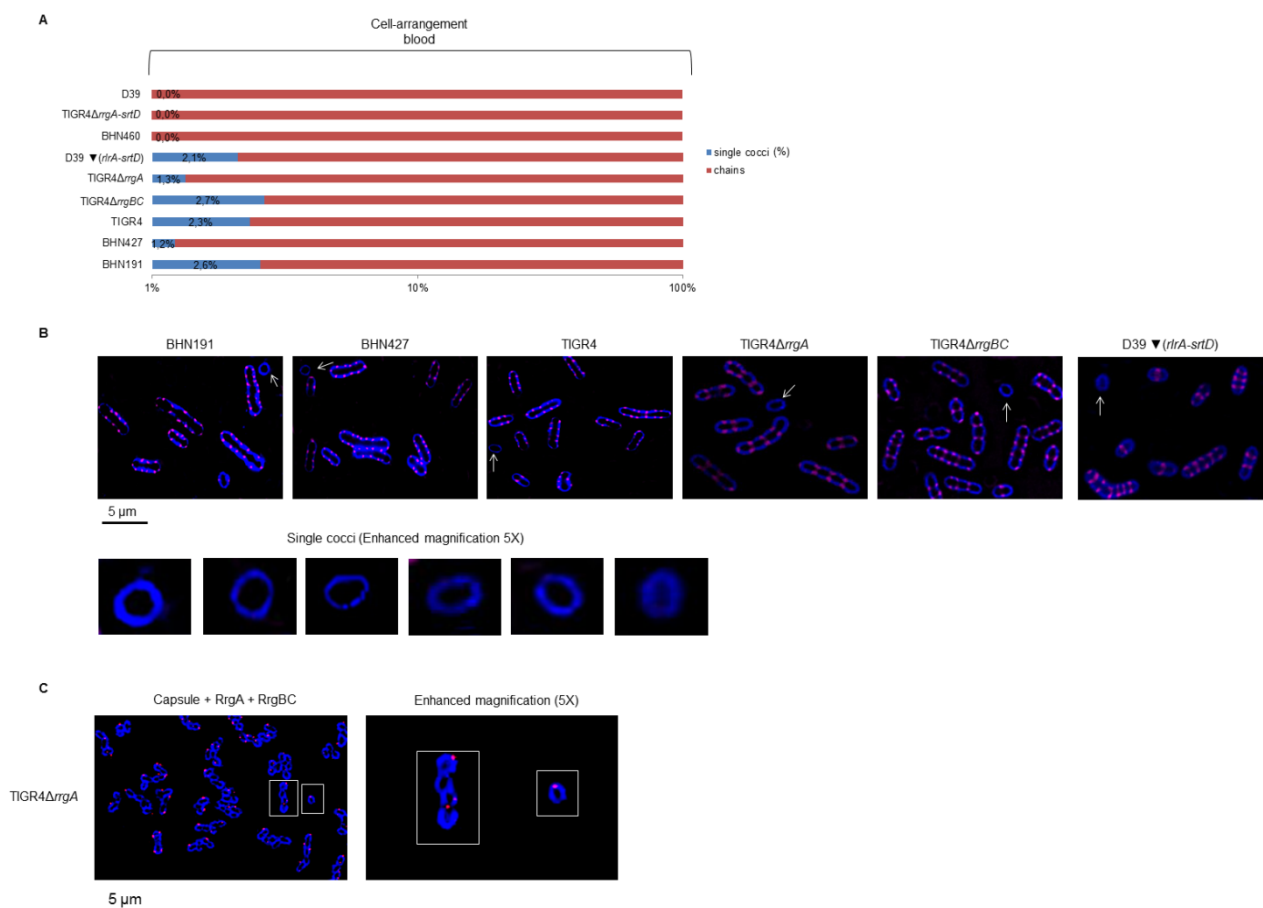


Supplemental Figure 12. Piliated single cocci express DivIVA only during cell division.

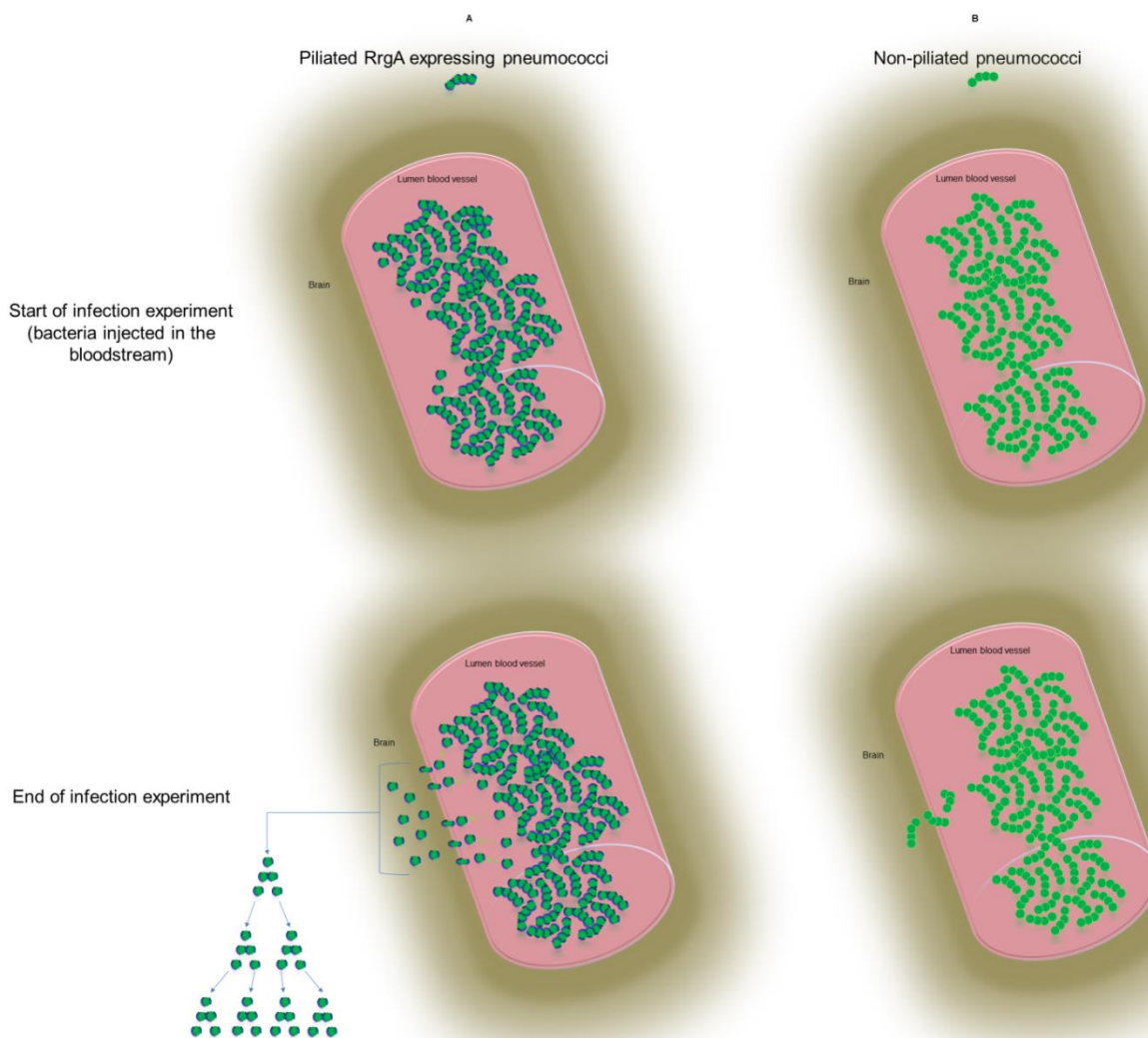
Immunofluorescent stainings of piliated pneumococci from brain homogenates showing capsule (blue) and DivIVA (red). (A) In the early stage of cell division bacteria started to show a division septum and the bacterial shape was still rounder; at this stage DivIVA is mostly localized at the poles of the cell. (B) In the late stage of cell division bacterial shape is more elongated and the two daughter cells are almost formed; at this stage DivIVA is normally recruited to the septum, however, here DivIVA has almost disappeared. One representative dividing coccus/strain is shown, in total approximately 20 dividing cocci have been imaged for each strain.



Supplemental Figure 13. In blood piliated and RrgA expressing single cocci do not express DivIVA. (A) Percentages of single cocci in the blood for all strains used in this study; approximately 900 bacteria/strain were imaged and counted for calculating the percentage of single cocci in the blood. (B) Immunofluorescent staining of piliated pneumococci in blood samples showing capsule (blue) and DivIVA (red). The panel “single cocci” shows single cocci pointed by the white arrows with a higher magnification. Single cocci are the only bacteria that do not have a DivIVA signal; one representative image (showing a discrete number of bacteria with 100X objective) per each strain is shown, in total approximately 900 bacteria/strain were imaged. (C) Immunofluorescent staining of TIGR4 Δ *rrgA* in blood samples showing capsule (blue), RrgA (green) and RrgBC (red), the panel ”Enhanced magnification” shows the parts within white rectangles with higher magnification; TIGR4 Δ *rrgA* did not show a RrgA signal, as expected; one representative image per each strain is shown (100X objective) and in total approximately 900 bacteria/strain were imaged.



Supplementary Figure 14. Proposed model for brain invasion by piliated and non-piliated pneumococci. (A) Piliated pneumococci expressing the adhesin RrgA are present in the blood mainly as chains, only a minor part (<5%) is in the form of single cocci. However, those single cocci are more prone to penetrate the blood-brain barrier (BBB) because of their small size and the presence of the pilin protein RrgA. Once in the brain these single cocci retain their ability to grow and divide. Constant seeding the BBB with circulating single cocci from the blood stream likely contributes to their accumulation in the brain (B) Non-piliated pneumococci not expressing the RrgA adhesin are present in the blood only as chains and no single cocci are observed. The chains, because of their size, are less capable than single cocci to penetrate the BBB. Furthermore, absence of the pilin protein RrgA reduces their adhesive capacity to the endothelium.



Supplemental Information

The insertion of 10bp (ATACTATACT) in BHN191 upstream of the translational start site for the *rrgA* gene

The position of the 10 bp insertion in BHN191 is located between the inversely transcribed *rlrA* and *rrgA* genes. The transcriptional data we obtained and previously published data (25) on the location of the promoter regions of both *rlrA* and *rrgA* argues against the implication of this insertion in modulating expression of the pilus as discussed below:

The insertion is located 252 bp upstream the *rlrA* +1 which is probably too far to affect its transcription, since it does not overlap the +1 or the -10 and -35 boxes. If it indeed affected transcription of *rlrA*, we would expect one of two possible scenarios: 1) up-regulation of *rlrA* and corresponding downregulation of the other pilus genes (this is not the case according to our qPCR data which shows that all pilus genes are more highly expressed in BHN191 than in BHN427) or 2) down-regulation of *rlrA* (which is not the case, since our qPCR data shows that *rlrA* is significantly more expressed in BHN191 than in 427).

The insertion is located 13 bp downstream the +1 of *rrgA*, so outside of the -10 and -35 boxes also in this case. If anything, it could decrease expression of *rrgA* by increasing the distance between the +1 and the ATG, but this is not the case, since *rrgA* is more highly expressed in BHN191 than in BHN427.

More probably this insertion results from a tandem duplication, since it is an almost exact repetition of a 10 bp sequence present twice immediately downstream the insertion in BHN191.

Quantification of single cocci/diplococci/chains in the brain (related to the data shown in Figure 2)

In the brain among piliated strains only a minor part formed diplococci. BHN191: 31 out of 900 bacteria imaged; TIGR4: 39 out of 900 bacteria imaged; D39▼(*rlrA-srtD*): 36 out of 900 bacteria imaged, and non-piliated, but RrgA containing, TIGR4Δ*rrgBC*: 41 out of 900 bacteria imaged, and no chains were observed. In contrast, non-piliated BHN460, TIGR4Δ*rrgA-srtD*, and D39 formed chains in the brain and single cocci were never detected among 900 bacteria imaged.

The piliated carriage isolate BHN427 and the piliated TIGR4 mutant TIGR4Δ*rrgA* showed a heterogeneous population of *single cocci* (BHN427: 334 out of 900 bacteria imaged; TIGR4Δ*rrgA*: 378 out of 900 bacteria imaged), *diplococci* (BHN427: 358 out of 900; TIGR4Δ*rrgA*: 397 out of 900 bacteria imaged) and *chains* (BHN427: 228 out of 900; TIGR4Δ*rrgA*: 125 out of 900 bacteria imaged).

Supplemental Methods

Pneumococcal strains and growth conditions

The three clinical isolates of serotype 6B, BHN191, BHN460 and BHN427 (3), the serotype 4 isolate TIGR4 and its isogenic mutants in TIGR4 Δ *rrgA-srtD*, TIGR4 Δ *rrgBC* and TIGR4 Δ *rrgA* (12), the serotype 2 D39 and its isogenic mutant complemented with *rlrA* genetic islet D39 ∇ (*rlrA-srtD*) (12) were used in this study. Pneumococci were grown upright without shaking in Todd-Hewitt broth with 0.5% yeast extract (THY) at 37°C and bacterial growth was monitored by measuring the optical density (OD) at 600 nm with a spectrophotometer. At OD₆₀₀ = 0.25-0.30 bacteria were harvested and collected in 1 ml aliquots. Aliquots were centrifuged at 10000 rpm for 3 minutes and the pellet resuspended in 1 ml of sterile phosphate-buffered saline (PBS). Serial dilutions in sterile PBS were plated on blood-agar plates to determine the dilutions required for 10⁷ CFU and 5x10⁶ CFU for intravenous and intranasal challenges, respectively.

Bioinformatic analysis

The serotype 6B isolates BHN191, BHN460, and BHN427 were sequenced using the Illumina Miseq platform and paired end sequencing with insert sizes of 250 bp and the Illumina Truseq library preparation kit attaining a minimum coverage of 100X per base. The reads were demultiplexed (Phred33/Sanger/Illumina 1.8+ encoding), adapters removed and quality trimmed using Trimmomatic. The genomes were *de novo* assembled using spades assembler and were aligned to each other using Burrows-Wheeler Aligner. For the pilus comparison, the quality trimmed reads of BHN460 and BHN427 were aligned to the pilus region of BHN191.

Mouse experiments

The bacteremia-derived meningitis model described by Iovino *et al.* (6, 7, 15) was performed with groups of 5 male C57BL/6 wild-type mice 5 to 6 weeks old (Charles River Laboratories Germany) that were anesthetized by inhalation of isoflurane (Abbott, catalog B506) before challenge. 200 μ l of 10^7 CFU were injected intravenously into the tail and the mice were sacrificed at 14 hours after bacterial challenge. After sacrifice, unattached bacteria in the blood stream were removed by perfusion with sterile PBS in the right ventricle via the vena cava until complete blood removal. The pneumonia model was performed by intranasal administration of 50 μ l of 5×10^6 CFU bacteria and mice were sacrificed at 24 hours post-infection. After harvesting, one half of the brain was cryopreserved and stored with Shandon Cryomatrix (Thermo Scientific, catalog 6769006) at -80°C while the other half was used to prepare homogenate samples (see *Preparation of mouse tissue homogenates and Western blot experiments*); of each pair of lungs, one lung was cryopreserved and one was used to prepare homogenate samples.

Antibodies and isotype controls

Immunofluorescent detection was performed using antibody combinations diluted in sterile PBS with 5% Fetal Calf Serum (FCS) (Biochrom, catalog S0115), as follows. *S. pneumoniae* anti-capsule serotype 4 and serotype 6B antibodies (Statens Serum Institut, Copenhagen, Denmark, catalogues 16924 and 16747): 1:100 dilution, followed by Alexa Fluor 488 goat anti-rabbit antibody (Thermo Fisher Scientific - Invitrogen Life Technologies, catalog A21244) diluted 1:500. For the detection of pilus 1 by immunofluorescent staining, a mix of rabbit anti RrgA, RrgB and RrgC antisera (Innovagen AB, RrgA catalog 302-315, RrgB catalog 393-406, RrgC catalog 192-205) was used. When capsule staining was combined with staining of the

three pilus proteins RrgA, RrgB, and RrgC, the anti-capsule antibodies were labeled with Alexa Fluor 350 fluorophore using the Zenon Rabbit IgG Labeling Kit (Thermo Fisher Scientific - Invitrogen Life Technologies, catalog Z25300) to a final dilution of 1:100. A mix of rabbit anti RrgA, RrgB and RrgC antisera was labeled with Alexa Fluor 488 fluorophore using the Zenon Rabbit IgG Labeling Kit (Thermo Fisher Scientific - Invitrogen Life Technologies, catalog Z25302) to a final dilution of 1:50; for RrgA (alone) detection anti RrgA antiserum was labeled with Alexa Fluor 488 using the Zenon Rabbit IgG Labeling Kit to a final dilution of 1:50; for RrgB and RrgC detection a mix of anti RrgB and RrgC antisera was labeled with Alexa Fluor 594 using the Zenon Rabbit IgG Labeling Kit (Thermo Fisher Scientific - Invitrogen Life Technologies, catalog Z25307) to a final dilution of 1:50. DivIVA and FtsZ were detected with rabbit anti DivIVA and anti FtsZ antisera (gift from Prof. Orietta Massidda, University of Cagliari, Italy); rabbit anti DivIVA antiserum and rabbit anti-FtsZ antibody were labeled with Alexa Fluor 594 fluorophore using the Zenon Rabbit IgG Kit to a final dilution of 1:100. Blood-brain barrier endothelium: DyLight 594-labeled LEL (Vector Laboratories, catalog DL-1177) diluted 1:200 (15). Lung epithelial cells: rabbit anti-cytokeratin (CK) 8 antibody (Nordic Biosite, catalog bs-1339R) was labeled with Alexa Fluor 594 fluorophore using the Zenon Rabbit IgG Labeling Kit to a final dilution of 1:100. Microglia: rabbit anti-ionized calcium-binding adapter molecule 1 (Iba-1) (Wako, catalog 019-19741) diluted 1:100 followed by Alexa Fluor 488 donkey anti-goat antibody (Thermo Fisher Scientific - Invitrogen Life Technologies, catalog A-11055) diluted 1:500. Anti avi-Tag antibody (GenScript, catalog A00674, rabbit IgG isotype control) was used as isotype control for the primary antibodies. Avi-Tag antibody was used in combination with Alexa Fluor 488 goat anti-rabbit antibody and no fluorescence was detected (data not shown). Incubation of mouse tissue sections with only the secondary antibodies was performed as additional control and did not result in a fluorescent signal (data not shown).

Antibodies used for Western blot experiments were diluted in PBS+0,1% Tween 20 (Sigma Aldrich, catalog P1379) (PBS-T) supplemented with 1% dry milk. Pneumolysin loading control was detected using a mouse anti pneumolysin antibody (Abcam, catalog ab71810) diluted 1:1000. RlrA pilus proteins were detected with rabbit anti RrgA, RrgB and RrgC antisera (gift from Novartis GSK Vaccines, Siena, Italy) diluted 1:1000. DivIVA was detected using the same antibody used for immunofluorescent staining, diluted 1:2000. Horseradish peroxidase conjugated Goat anti-Mouse IgG and Goat anti-Rabbit IgG (GE Healthcare, catalogues NXA931 and RPN4301) diluted 1:5000 were used as secondary antibodies for the detection of Mouse IgGs and Rabbit IgGs, respectively.

Immunofluorescent detection and microscopy imaging

5 µm thick brain and lung sections were cut with a cryostat and placed on microscope glass slides (3 sections/slide) (VWR, catalog 631-1551). Sections were fixed with acetone for 10 minutes, dried and incubated with the anti-capsule antibody for 1 hour. Slides were washed twice in PBS for 5 minutes and each section was then incubated with the appropriate secondary antibody for 1 hour in the dark and washed again twice in PBS for 5 minutes. Slides were then incubated in the dark for 45 minutes with DyLight 594-labeled LEL (brain) or labeled anti-CK8 antibody (lungs). The slides were then washed in PBS, and Vectashield solution (Vector Laboratories, catalog H-1400) was added to each section before the coverslip was applied. 30 µm thick brain sections were used for microglia detection. Slides were fixed with acetone, incubated with the anti-Iba-1 antibody overnight at 4°C and washed in PBS 3 times for 5 minutes. The slides were then incubated 2 hours in the dark with the appropriate secondary antibody.

For the detection of capsule, pilus 1 and DivIVA from THY cultures, blood samples, lung and brain homogenate samples (see *Preparation of mouse tissue homogenates and Western blot experiments*) were collected in 250 µl aliquots. Each aliquot was centrifuged at 10000 rpm for 5 minutes, the pellet resuspended in 100 µl of labeled anti RrgABC antisera and incubated at 4°C for 1 hour in the dark. The pellet was washed twice with PBS-T, then resuspended with the labeled anti DivIVA antibody and incubated at 4°C for 1 hour in the dark. The pellet was washed again twice with PBS-T and resuspended with the labeled anti-capsule antibody. After final wash in PBS, the pellet was resuspended in 100 µl of distilled water and 10 µl drops were pipetted onto a microscope glass slide and dried. Vectashield (Vector Laboratories) was finally added to each dried drop, covered with a coverslip and analyzed by fluorescence microscopy. Microscopy was performed using a DV Elite microscope (Applied Precision) using a scientific complementary metal-oxide-semiconductor (sCMOS) camera. Images were acquired using Softworx (Applied Precision).

Bacterial quantification in immunofluorescent images

Bacterial signal quantification in fluorescent images acquired at low magnification (10X objective) was performed as previously described (15). Briefly, using the *Threshold* function of Image J (26) the surface covered by bacteria and by the brain vasculature were measured to determine the area occupied by the 488 nm (bacteria) signal and 594 nm (brain vasculature/brain tissue) signals, respectively. The bacteria to brain tissue ratio was calculated by dividing the surface of the 488 nm signal by the total area of the tissue detected in each image.

Preparation of mouse tissue homogenates and Western blot experiments

After harvesting, mouse organs were kept in 1 ml sterile PBS and homogenized using a cell strainer with 100 µm filter (Falcon, catalog 08-77119). Homogenates were centrifuged at 12000 rpm for 5 minutes and the pellet was resuspended in 1X LDS-sample buffer (Thermo Fisher Scientific – Invitrogen Life Technologies, catalog NP0007) and boiled at 95°C for 5 minutes. Quality of each tissue homogenate was assessed by SDS-page following Coomassie staining. Tissue homogenate lysates were loaded onto a 10% NuPage Novex Bis-Tris Gel (Thermo Fisher Scientific – Invitrogen Life Technologies, catalog NP0302BOX) and the electroblotting was performed using the Biorad Trans-Blot Turbo Transfer System (Biorad).

Quantification of protein expression

Density of protein bands on Western blot membranes were measured with Image J (7,26). Rectangles were drawn around each protein band, the intensity of pixels from the top of the rectangle to the bottom of the rectangle was generated and the areas of each peak of pixel intensity were calculated. Protein signal values (RrgA, RrgB, RrgC and DivIVA) were corrected for the pneumolysin loading control.

RNA isolation and quantitative reverse transcriptase PCR

Bacteria were grown in C+Y/10%DS until $OD_{620}=0.5$. The RNA was stabilized with 2/5 v:v 95% EtOH and 5% phenol, followed by 30 minute incubation on ice. Bacterial cells were harvested by centrifugating 2 min at 16000 g at 4°C. RNA was extracted using Trizol/phenol as described previously (27). DNA in samples was removed using DNase Turbo (Thermo Fisher Scientific - Ambion, catalog AM2222) and RNA was extracted using

Phenol:Chloroform:Isoamyl alcohol (25:24:1, Sigma Aldrich, catalog P2069). RNA integrity was validated by gel electrophoresis, and successful DNA removal by PCR. RNA was converted into cDNA using Multiscribe Reverse Transcriptase according to the manufacturer's instruction (Thermo Fisher Scientific – Ambion, catalog 4311235) and the levels of target and endogenous control genes were assayed by qPCR using the iTaq™Universal SYBR®Green Supermix (Biorad, catalog 1725121), reaction composition and protocol according to the manufacturer's instruction. Relative gene expression values were calculated using the $2^{-\Delta\Delta CT}$ algorithm, normalizing to the house-keeping gene *GAPDH* (28).

References (cited only in the Supplemental Information and Supplemental Methods)

25. Hava DL, Hemsley CJ, Camilli A. Transcriptional regulation in the *Streptococcus pneumoniae* *rlrA* pathogenicity islet by RlrA. *J Bacteriol.* 2003;185(2):413-21.
26. Schneider CA, Rasband WS, Eliceiri KW. NIH Image to ImageJ: 25 years of image analysis. *Nat Methods.* 2012;9(7):671–5.
27. Kröger C, et al. The transcriptional landscape and small RNAs of *Salmonella enterica* serovar Typhimurium. *Proc Natl Acad Sci U S A.* 2012;109(29):E1277-86.
28. Livak KJ, Schmittgen TD. Analysis of relative gene expression data using real-time quantitative PCR and the $2^{-\Delta\Delta C(T)}$ Method. *Methods.* 2001;25(4):402-8.